Monthly Notices
of the
ROYAL ASTRONOMICAL SOCIETY

Mon. Not. R. Astron. Soc. **413,** 2583–2594 (2011) doi:10.1111/j.1365-2966.2011.18326.x

Optical studies of SN 2009jf: a Type Ib supernova with an extremely slow decline and aspherical signature

D. K. Sahu,[1⋆] U. K. Gurugubelli,[1,2⋆] G. C. Anupama[1⋆] and K. Nomoto[3⋆]

[1]*Indian Institute of Astrophysics, Koramangala, Bangalore 560034, India*
[2]*Joint Astronomy Programme, Indian Institute of Science, Bangalore 560012, India*
[3]*Institute for the Physics and Mathematics of the Universe, University of Tokyo, Kashiwa, Chiba 277-8583, Japan*

Accepted 2011 January 10. Received 2011 January 7; in original form 2010 September 13

ABSTRACT

Optical *UBVRI* photometry and medium-resolution spectroscopy of the Type Ib supernova SN 2009jf, during the period from ~ -15 to $+250$ d, with respect to the *B* maximum are reported. The light curves are broad, with an extremely slow decline. The early post-maximum decline rate in the *V* band is similar to SN 2008D; however, the late-phase decline rate is slower than other Type Ib supernovae studied. With an absolute magnitude of $M_V = -17.96 \pm 0.19$ at peak, SN 2009jf is a normally bright supernova. The peak bolometric luminosity and the energy deposition rate via the $^{56}\mathrm{Ni} \rightarrow {}^{56}\mathrm{Co}$ chain indicate that $\sim 0.17^{+0.03}_{-0.03}\,\mathrm{M}_\odot$ of ^{56}Ni was ejected during the explosion. The He I 5876 Å line is clearly identified in the first spectrum of day ~ -15, at a velocity of $\sim 16\,000\,\mathrm{km\,s^{-1}}$. The [O I] 6300–6364 Å line seen in the nebular spectrum has a multipeaked and asymmetric emission profile, with the blue peak being stronger. The estimated flux in this line implies that $\gtrsim 1.34\,\mathrm{M}_\odot$ oxygen was ejected. The slow evolution of the light curves of SN 2009jf indicates the presence of a massive ejecta. The high expansion velocity in the early phase and broader emission lines during the nebular phase suggest it to be an explosion with a large kinetic energy. A simple qualitative estimate leads to the ejecta mass of $M_{\mathrm{ej}} = 4$–$9\,\mathrm{M}_\odot$ and kinetic energy $E_{\mathrm{K}} = 3$–8×10^{51} erg. The ejected mass estimate is indicative of an initial main-sequence mass of $\gtrsim 20$–$25\,\mathrm{M}_\odot$.

Key words: supernovae: general – supernovae: individual: SN 2009jf – galaxies: individual: NGC 7479.

1 INTRODUCTION

Type Ib supernovae (SNe Ib) are core-collapse supernovae, characterized by the presence of prominent helium lines and the absence of hydrogen lines. They are believed to be the results of violent explosions of massive stars, such as the Wolf–Rayet stars, which are stripped of most or all of their hydrogen envelope, either by mass transfer to a companion (e.g. Nomoto et al. 1993; Podsiadlowski et al. 2004), or via strong winds (e.g. Woosley, Langer & Weaver 1993) or by sudden eruptions. These supernovae are also termed as stripped-envelope supernovae.

The presence of hydrogen in SNe Ib remains an open issue for investigation. There are some Type Ib events which show a deep absorption at ∼6200 Å in their early spectra, which could be attributed to Hα (Branch et al. 2002; Anupama et al. 2005; Soderberg et al. 2008), whereas some others show a shoulder in the red wing of the [O I] 6300–6364 Å line in their nebular spectra, due to Hα (Sollerman, Leibundgut & Spyromilio 1998; Stritzinger et al. 2009). Using the SYNOW code, Elmhamdi et al. (2006) have shown the presence of a thin layer of hydrogen ejected at high velocity in almost all the SNe Ib in their sample. Maurer et al. (2010) have recently investigated various mechanisms that can produce strong Hα emission in the late phase and showed that it can be well explained by radioactive energy deposition, if hydrogen and helium are mixed in suitable fractions and clumped strongly.

Late-phase observations of SNe Ib have gained special importance as these phases probe deeper into the core of the expanding stars. The nebular spectrum originating from an optically thin ejecta provides important clues to the nature of the progenitor star and the explosion mechanism. Asphericity in the explosion of stripped envelope supernovae is confirmed by a higher degree of polarization through spectropolarimetric studies of these objects during early phases (Wang et al. 2003; Leonard et al. 2006). Independent indications of the asphericity in the explosion come from the narrower width of the [O I] 6300–6364 Å line compared to the [Fe II] features at ∼5200 Å (Mazzali et al. 2001; Maeda et al. 2002) and/or from the asymmetric profile of the [O I] 6300–6364 Å line (Mazzali et al. 2005).

⋆E-mail: dks@iiap.res.in (DKS); uday@iiap.res.in (UKG); gca@iiap.res.in (GCA); nomoto@astron.s.u-tokyo.ac.jp (KN)

SN 2009jf was discovered by Li, Cenko & Filippenko (2009) in the Seyfert 2, barred spiral galaxy NGC 7479 on September 27.33. This supernova was classified as a young SN Ib by Kasliwal et al. (2009) and Sahu, Anupama & Gurugubelli (2009a), based on early spectra obtained on September 29. Itagaki, Kaneda & Yamaoka (2009) reported the detection of a dim object at an unfiltered magnitude of ∼18.2 in an image obtained on 2006 November 8.499 and at a magnitude of ∼18.3 in an image obtained on 2007 August 13.74. They also reported the presence of the object at ∼18 mag in the Digitized Sky Survey (DSS) images. They have estimated the absolute magnitude of the object as −14.5 and suggested that these may be recurring outbursts of a luminous blue variable.

In this paper, we report optical photometry and spectroscopy of SN 2009jf in the early and nebular phases and discuss the results based on the observations.

2 OBSERVATION AND DATA REDUCTION

2.1 Photometry

Photometric observations of SN 2009jf began on 2009 September 29, using the 2-m Himalayan Chandra Telescope (HCT) of the Indian Astronomical Observatory, immediately after discovery, and continued until 2010 June 21, with a break during the period the supernova was behind the Sun. The observations were made using the Himalaya Faint Object Spectrograph Camera (HFOSC). The central 2K × 2K region of the 2K × 4K SITe CCD chip in use with HFOSC was used for imaging. This provides an image scale of 0.296 arcsec pixel^{-1} over a 10 × 10 arcmin^2 field of view. Further details on the telescope and instrument can be obtained from http://www.iiap.res.in/centers/iao. The supernova was observed in Bessell *U*, *B*, *V*, *R* and *I* filters. Standard fields PG 0231+051, PG 1657+078 and PG 2213−006 (Landolt 1992), observed under the photometric sky condition on 2009 September 30 and October 14, are used for photometric calibration of the supernova magnitudes.

Data reduction was done in the standard manner; the data were bias subtracted, flat-fielded and cosmic ray hits removed, using the standard tasks available within the Image Reduction and Analysis Facility (IRAF) package. Aperture photometry was performed on the standard stars with an optimal aperture determined using the aperture growth curve method. Aperture correction between the optimal aperture and an aperture close to the full width at half-maximum (FWHM) of the stellar profile that had the maximum signal-to-noise ratio was determined using the brighter stars and then applied to the fainter ones. Average extinction values for the site (Stalin et al. 2008) were used to correct for the atmospheric extinction and the average colour terms for the filter-detector system were used to get the photometric solutions, based on the magnitudes of the stars in the standard fields. These were then used to calibrate a sequence of local standards in the supernova field observed on the same nights as the standard fields. The local standards were then used for the photometric calibration of the supernova magnitudes. The magnitudes of the local standards in the supernova field are listed in Table 1 and the supernova field with the local standards marked is shown in Fig. 1. The magnitudes of the supernova and the secondary standards were estimated using point-spread function photometry, with a fitting radius equal to the FWHM of the stellar profile. The difference between the aperture and profile fitting photometry was estimated using bright standards in the field and applied to the supernova magnitude. The night-to-night zero-points were estimated using the local standards in the supernova field and the supernova magnitudes calibrated differentially with respect to

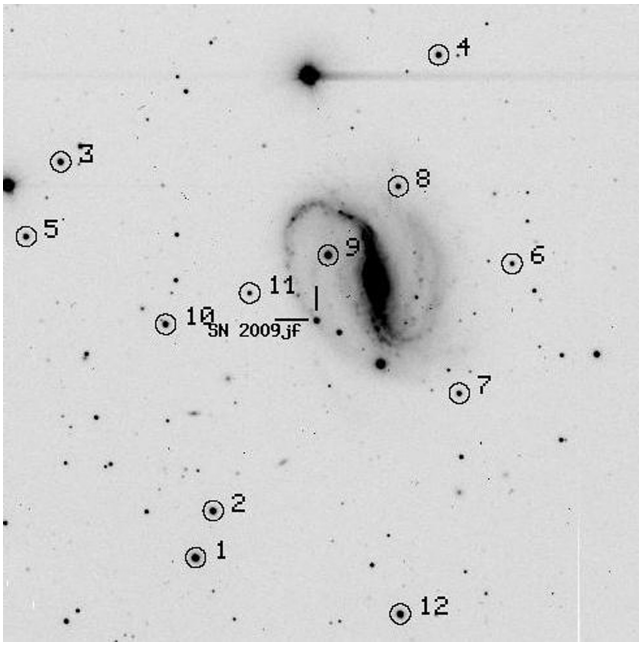

Figure 1. Identification chart for SN 2009jf. The stars used as local standards are marked with numbers 1–12. South is up and east to the right. The field of view is 10 × 10 arcmin^2.

Table 1. Magnitudes for the sequence of secondary standard stars in the field of SN 2009jf.

ID	*U*	*B*	*V*	*R*	*I*
1	14.846 ± 0.063	14.717 ± 0.010	14.052 ± 0.019	13.639 ± 0.003	13.218 ± 0.016
2	16.260 ± 0.087	15.757 ± 0.006	14.878 ± 0.015	14.340 ± 0.011	13.834 ± 0.006
3	16.197 ± 0.079	15.885 ± 0.004	15.148 ± 0.024	14.739 ± 0.001	14.317 ± 0.013
4	16.366 ± 0.061	16.040 ± 0.005	15.289 ± 0.011	14.849 ± 0.010	14.421 ± 0.020
5	16.228 ± 0.082	16.156 ± 0.006	15.463 ± 0.023	15.061 ± 0.002	14.620 ± 0.012
6	19.942 ± 0.181	18.271 ± 0.010	16.915 ± 0.014	16.071 ± 0.005	15.320 ± 0.013
7	18.775 ± 0.096	17.387 ± 0.001	16.203 ± 0.017	15.475 ± 0.003	14.860 ± 0.016
8	17.128 ± 0.077	16.729 ± 0.004	15.939 ± 0.022	15.455 ± 0.000	14.996 ± 0.021
9	16.054 ± 0.059	15.350 ± 0.021	14.464 ± 0.030	13.958 ± 0.000	13.519 ± 0.019
10	16.446 ± 0.057	16.088 ± 0.005	15.266 ± 0.024	14.764 ± 0.004	14.264 ± 0.017
11	17.209 ± 0.094	17.182 ± 0.007	16.555 ± 0.015	16.139 ± 0.009	15.720 ± 0.012
12	15.440 ± 0.065	15.332 ± 0.010	14.659 ± 0.020	14.232 ± 0.005	13.791 ± 0.012

Table 2. Photometric observations of SN 2009jf.

Date	JD 245 4000+	Phase[a] (d)	*U*	*B*	*V*	*R*	*I*
2009/09/29	245 5104.171	−15.29	17.557 ± 0.030	17.622 ± 0.020	17.047 ± 0.019	16.733 ± 0.024	16.578 ± 0.027
2009/09/30	245 5105.173	−14.29	17.168 ± 0.067	17.275 ± 0.026	16.739 ± 0.023	16.443 ± 0.016	16.317 ± 0.016
2009/10/01	245 5106.104	−13.36	16.945 ± 0.033	16.990 ± 0.037	16.508 ± 0.025	16.219 ± 0.026	16.077 ± 0.019
2009/10/03	245 5108.261	−11.20		16.441 ± 0.032	16.001 ± 0.038	15.774 ± 0.031	15.594 ± 0.032
2009/10/04	245 5109.194	−10.27	16.078 ± 0.040	16.275 ± 0.035	15.842 ± 0.034	15.611 ± 0.032	15.458 ± 0.028
2009/10/08	245 5113.119	−6.34	15.572 ± 0.043	15.752 ± 0.032	15.365 ± 0.012	15.159 ± 0.013	14.980 ± 0.026
2009/10/14	245 5119.308	−0.15	15.582 ± 0.042	15.594 ± 0.021	15.092 ± 0.011	14.857 ± 0.015	14.643 ± 0.010
2009/10/15	245 5120.120	+0.66	15.517 ± 0.028	15.575 ± 0.025	15.078 ± 0.019	14.826 ± 0.024	14.638 ± 0.020
2009/10/16	245 5121.313	+1.85	15.580 ± 0.044	15.618 ± 0.027	15.082 ± 0.014	14.816 ± 0.015	14.600 ± 0.037
2009/10/22	245 5127.171	+7.71	15.992 ± 0.035	15.855 ± 0.011	15.136 ± 0.009	14.832 ± 0.020	14.588 ± 0.025
2009/10/24	245 5129.265	+9.81	16.153 ± 0.030	15.988 ± 0.016	15.186 ± 0.020	14.864 ± 0.023	14.597 ± 0.025
2009/10/27	245 5132.288	+12.83	16.574 ± 0.039	16.277 ± 0.028	15.318 ± 0.024	14.950 ± 0.034	14.649 ± 0.038
2009/10/31	245 5136.187	+16.73		16.687 ± 0.027	15.604 ± 0.029	15.132 ± 0.024	14.777 ± 0.021
2009/11/06	245 5142.047	+22.59		17.118 ± 0.018	15.933 ± 0.021	15.403 ± 0.021	15.024 ± 0.044
2009/11/10	245 5146.146	+26.69	17.534 ± 0.056	17.291 ± 0.018	16.108 ± 0.019	15.565 ± 0.013	15.138 ± 0.043
2009/11/14	245 5150.057	+30.60	17.598 ± 0.087	17.421 ± 0.031	16.268 ± 0.012	15.720 ± 0.020	15.246 ± 0.014
2009/11/17	245 5153.156	+33.70		17.454 ± 0.013	16.353 ± 0.022	15.823 ± 0.017	15.328 ± 0.029
2009/11/21	245 5157.21	+37.75		17.547 ± 0.020	16.455 ± 0.017	15.946 ± 0.021	15.439 ± 0.019
2009/11/25	245 5161.048	+41.59		17.603 ± 0.025	16.510 ± 0.032	16.026 ± 0.031	15.537 ± 0.034
2009/11/30	245 5166.188	+46.73		17.647 ± 0.032	16.594 ± 0.034	16.116 ± 0.024	15.596 ± 0.017
2009/12/03	245 5169.030	+49.57		17.654 ± 0.031	16.624 ± 0.014	16.173 ± 0.032	15.653 ± 0.031
2009/12/18	245 5184.040	+64.58		17.751 ± 0.020	16.815 ± 0.020	16.393 ± 0.016	15.855 ± 0.023
2009/12/23	245 5189.036	+69.58		17.812 ± 0.033	16.890 ± 0.017	16.478 ± 0.025	15.964 ± 0.029
2009/12/29	245 5195.151	+75.69		17.847 ± 0.024	16.947 ± 0.028	16.541 ± 0.012	16.061 ± 0.045
2010/01/09	245 5206.041	+86.58		17.887 ± 0.022	17.079 ± 0.021	16.692 ± 0.022	16.213 ± 0.043
2010/01/20	245 5217.073	+97.61		18.003 ± 0.020	17.203 ± 0.019	16.819 ± 0.016	16.326 ± 0.016
2010/01/27	245 5224.073	+104.61		18.151 ± 0.040	17.295 ± 0.036	16.946 ± 0.012	16.464 ± 0.020
2010/02/01	245 5229.071	+109.61		18.181 ± 0.049	17.410 ± 0.019	17.011 ± 0.014	16.563 ± 0.016
2010/05/01	245 5318.442	+198.98			18.524 ± 0.038	17.979 ± 0.025	17.785 ± 0.033
2010/05/24	245 5341.418	+221.96		19.212 ± 0.046	18.753 ± 0.024	18.126 ± 0.022	18.013 ± 0.039
2010/05/26	245 5343.406	+223.95		19.296 ± 0.029	18.808 ± 0.031	18.177 ± 0.052	18.019 ± 0.051
2010/06/11	245 5359.430	+239.97		19.456 ± 0.034	19.075 ± 0.032	18.427 ± 0.036	18.336 ± 0.038
2010/06/21	245 5369.353	+249.89		19.462 ± 0.028	19.109 ± 0.026	18.539 ± 0.026	18.373 ± 0.034

[a]Observed phase with respect to the epoch of maximum in the *B* band (JD 245 5119.46).

the local standards. The supernova magnitudes in *U*, *B*, *V*, *R* and *I* bands are given in Table 2.

2.2 Spectroscopy

Spectroscopic observations of SN 2009jf were obtained during 2009 September 29 (JD 245 5104.16) and 2010 June 22 (JD 245 5370.38). The spectra were obtained in the wavelength ranges of 3500–7800 and 5200–9250 Å using grisms Gr7 and Gr8 available with HFOSC. The log of spectroscopic observations is given in Table 3. Arc lamp spectra of FeNe and FeAr were obtained for wavelength calibration. Spectroscopic data reduction was performed in the standard manner. All spectra were bias subtracted, flat-fielded and the one-dimensional spectra extracted using the optimal extraction method (Horne 1986). Wavelength calibration was effected using the arc lamp spectra. The accuracy of wavelength calibration was checked using the night sky emission lines, and whenever necessary small shifts were applied to the observed spectra. The spectra were flux calibrated by correcting for the instrumental response using response curves estimated from the spectra of spectrophotometric standards that were observed on the same night. For the nights that standard star spectra were not available, the response curve obtained during observations on nearby nights was used. The flux-calibrated spectra in the two regions were then combined, scaled to a weighted mean to give the final spectrum. This spectrum was then brought to an absolute flux scale using zero-points determined from broad-band *UBVRI* magnitudes. The supernova spectra were corrected for the host galaxy redshift of $z = 0.007\,942$ and dereddened for a total reddening of $E(B - V) = 0.112$, as estimated in Section 4. The telluric lines have not been removed from the spectra.

Table 3. Log of spectroscopic observations of SN 2009jf.

Date	JD 245 0000+	Phase (d)	Range (Å)
2009/09/29	5104.16	−15.30	3500–7800; 5200–9250
2009/09/30	5105.13	−14.33	3500–7800; 5200–9250
2009/10/01	5106.17	−13.29	3500–7800; 5200–9250
2009/10/07	5112.09	−7.37	3500–7800; 5200–9250
2009/10/08	5113.07	−6.39	3500–7800; 5200–9250
2009/10/15	5120.17	+0.71	3500–7800; 5200–9250
2009/10/24	5129.22	+9.76	3500–7800; 5200–9250
2009/11/10	5146.19	+26.73	3500–7800; 5200–9250
2009/11/17	5153.17	+33.71	3500–7800; 5200–9250
2009/12/03	5169.17	+49.71	3500–7800; 5200–9250
2009/12/23	5189.06	+69.60	3500–7800; 5200–9250
2010/01/08	5205.04	+85.58	3500–7800; 5200–9250
2010/01/21	5218.07	+98.61	3500–7800; 5200–9250
2010/05/31	5348.40	+228.94	5200–9250
2010/06/22	5370.38	+250.92	5200–9250

3 OPTICAL LIGHT CURVES AND COLOUR CURVES

The light curves of SN 2009jf in the *UBVRI* bands are presented in Fig. 2. Also included in the figure are the unfiltered discovery magnitude and the pre-discovery limiting magnitudes (Li et al. 2009). Our observations began 2 d after discovery, ∼15 d before maximum in the *B* band, and continued till ∼250 d after maximum. The date of maximum brightness and the peak magnitude in different bands have been estimated by fitting a cubic spline to the points around maximum and are listed in Table 4. Similar to other Type Ib/c supernovae, the light curve of SN 2009jf peaks early in the bluer bands than in the redder bands. The maximum in *B* occurred on JD 245 5119.46 (2009 October 14.9), at an apparent magnitude of 15.56 ± 0.02.

The light curves of SN 2009jf are compared with those of a few well-studied core-collapse supernovae, namely SN 2008D (Modjaz et al. 2009), SN 2007Y (Stritzinger et al. 2009), SN 1999ex (Stritzinger et al. 2002), SN 1990I (Elmhamdi et al. 2004), broad-lined Type Ic SN 1998bw and the fast declining broad-lined Type Ic SN 2007ru (Sahu et al. 2009b), in Fig. 3. The observed magnitudes of the supernovae have been normalized to their respective peak magnitudes and shifted in time to the epoch of maximum brightness in the *B* band. From the figure, it is seen that the initial rise to maximum and post-maximum decline of SN 2009jf is slower in comparison with other supernovae, making the light curve of SN 2009jf broader. The post-maximum decline of the light curve

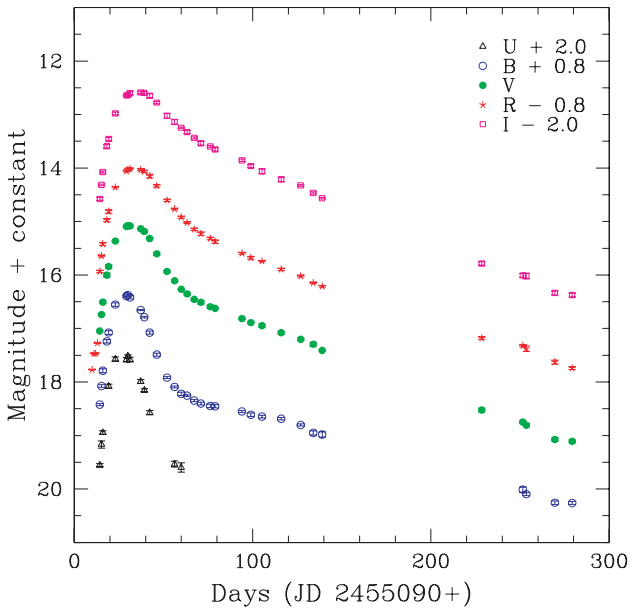

Figure 2. *UBVRI* light curves of SN 2009jf. The light curves have been shifted by the amount indicated in the legend.

Table 4. Light-curve maximum parameters.

Filter	JD at max. 245 5000+	Peak obs mag.	Peak abs mag.
U	116.60 ± 0.65	15.458 ± 0.014	−17.759 ± 0.19
B	119.46 ± 0.50	15.558 ± 0.020	−17.579 ± 0.19
V	120.98 ± 0.48	15.056 ± 0.022	−17.964 ± 0.19
R	121.44 ± 1.03	14.813 ± 0.032	−18.121 ± 0.19
I	124.10 ± 0.60	14.586 ± 0.010	−18.253 ± 0.19

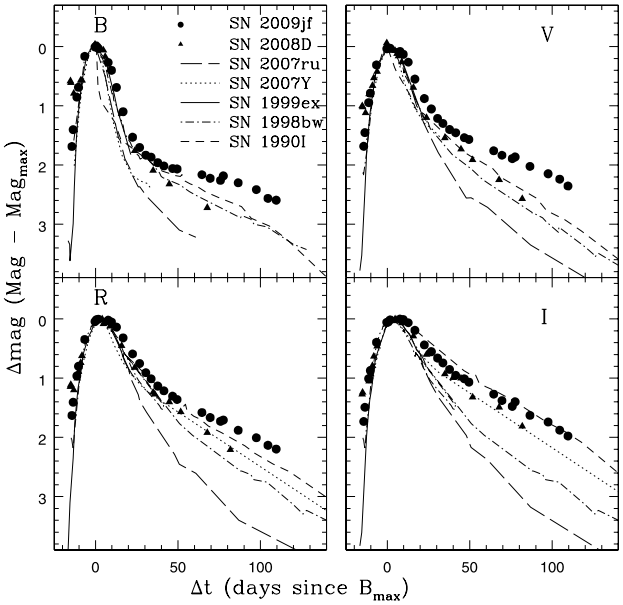

Figure 3. Comparison of *UBVRI* light curves of SN 2009jf with those of SN 2008D, SN 2007Y, SN 1999ex, SN 1990I, SN 1998bw and SN 2007ru. The light curves have been normalized as described in the text.

in 15 d, i.e. Δm_{15} estimated for different bands, is $\Delta m_{15}(U) = 0.971$, $\Delta m_{15}(B) = 0.908$, $\Delta m_{15}(V) = 0.503$, $\Delta m_{15}(R) = 0.311$ and $\Delta m_{15}(I) = 0.303$. These estimates indicate the decline rate in *V* to be similar to that of SN 2008D, but considerably slower than other SNe Ib and Ic. The decline rates estimated for the later phases (>40 d) are 0.008 mag d^{-1} in *B*, 0.0126 mag d^{-1} in *V*, 0.0141 mag d^{-1} in *R* and 0.0145 mag d^{-1} in *I*. These rates are slower in comparison with other SNe Ib. The broader light curves and slower decline rates suggest that the ejecta of SN 2009jf is relatively efficient in trapping the γ-rays produced in the radioactive decay. This also indicates that the progenitor of SN 2009jf was able to retain more of an envelope prior to the core-collapse, thus increasing the diffusion time for the energy produced from the radioactive decay of ^{56}Ni to ^{56}Co (Arnett 1982; Stritzinger et al. 2002).

There are only a few cases of SNe Ib where the rise time to the *B*-band maximum is constrained accurately. For example, the rise time for SN 1999ex and that for SN 2008D are found to be 18 d (Stritzinger et al. 2002) and 16.8 d (Modjaz et al. 2009), respectively. The rise time could be constrained for these two supernovae as they occurred in galaxies which were already being monitored to follow up other events. SN 1999ex was detected in IC 5179 which hosted SN 1999ee (Martin et al. 1999). The data obtained as a part of monitoring of SN 1999ee had the possible detection of the initial shock breakout due to SN 1999ex. Similarly, the shock breakout of SN 2008D was detected by the *Swift* satellite, as an X-ray transient XRT 080109, during a routine follow-up observation of SN 2007uy in NGC 2770 (Berger & Soderberg 2008). The peak of the X-ray transient is expected to occur shortly after the supernova explosion (Li 2007). SN 2009jf was discovered on September 27.33, around 17.5 d before maximum in the *B* band. Comparing with SN 1999ex and SN 2008D, it appears that SN 2009jf was most likely discovered almost immediately after explosion. However, since we are unable to constrain the shock breakout precisely, a rise time of 19 ± 1 d is assumed in this work.

The colour evolution of SN 2009jf is plotted in Fig. 4. The colour curves of SN 2008D, SN 2007Y and SN 1999ex are also included in

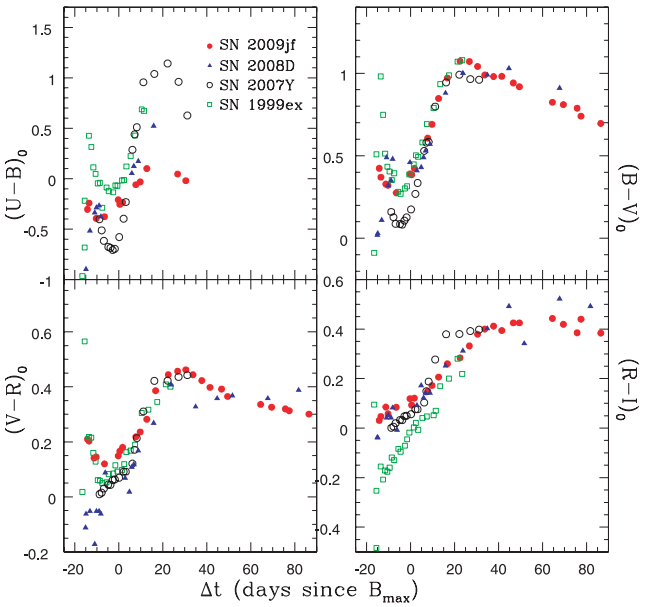

Figure 4. $(U-B)$, $(B-V)$, $(V-R)$ and $(R-I)$ colour curves of SN 2009jf compared with those of SN 2008D, SN 2007Y and SN 1999ex.

the figure for comparison. The colour curves have been corrected for total reddening values of $E(B-V)$ of 0.112 for SN 2009jf, 0.65 for SN 2008D (Mazzali et al. 2008), 0.112 for SN 2007Y (Stritzinger et al. 2009) and 0.3 for SN 1999ex (Stritzinger et al. 2002). The reported magnitudes of SN 2007Y are in the u', g', B, V, r' and i' bands. These magnitudes have been transformed to the *UBVRI* system using transformation equations given in Jester et al. (2005). The $(U-B)$, $(B-V)$ and $(V-R)$ colour curves of SN 2009jf evolve from red to blue in the pre-maximum epoch. This colour change can be attributed to an increase in the photospheric temperature with brightening of the supernova in the pre-maximum phase. The $(B-V)$ colour attains a value of 0.25 mag at ∼5 d before maximum in the B band; after that it monotonically becomes redder till ∼20 d after B maximum, indicating cooling due to envelope expansion. It again starts becoming blue at later epochs. The $(V-R)$ colour follows a similar trend, while the $(R-I)$ colour evolves towards red monotonically. The $(B-V)$ and $(V-R)$ colour evolution of SN 2009jf is quite similar to that of SN 1999ex, while the $(U-B)$ colour is always bluer and the $(R-I)$ colour redder than SN 1999ex. While SN 2009jf is redder than both SN 2007Y and SN 2008D in the pre-maximum epoch, the post-maximum colour evolution is similar in all three SNe, except for the $(U-B)$ colour, which remains bluer in SN 2009jf.

4 DISTANCE AND REDDENING

SN 2009jf is located at 54 arcsec west and 37 arcsec north of the nucleus of NGC 7479, at the edge of the outer arm of the host galaxy. From the infrared dust maps of Schlegel, Finkbeiner & Davis (1998), the Galactic interstellar reddening in the direction of NGC 7479 is $E(B-V)_{\rm Gal} = 0.112$ mag. The spectrum of SN 2009jf obtained close to maximum light shows the presence of weak Na I D absorption from the Milky Way. We do not detect any Na I D absorption due to the host galaxy. The low reddening of the supernova is also evident from its optical colours (see Fig. 4). We therefore conclude that there is no additional extinction due to the host galaxy and use a value of $E(B-V) = 0.112$ mag for extinction correction.

The radial velocity of NGC 7479, corrected for Local Group infall on to the Virgo Cluster, is 2443 km s^{-1} (Lyon/Meudon Extragalactic Database [LEDA]), which implies a distance modulus of 32.70 ± 0.18 for an H_0 value of 71 ± 6 km s^{-1} Mpc^{-1}. This leads to a distance of 34.66 ± 2.9 Mpc for NGC 7479. The errors in distance modulus and distance are estimated taking into account the uncertainty in H_0. The redshift-independent distance estimate using the Tully–Fisher relation is 33.85 ± 3.1 [NASA/IPAC Extragalactic Database (NED)], which is in close agreement with the distance estimates using the radial velocity. We use the mean of the two estimates, 34.25 ± 4.2 Mpc, as the distance to NGC 7479 for further analysis.

5 ABSOLUTE MAGNITUDE, BOLOMETRIC LIGHT CURVE AND MASS OF ^{56}NI

The absolute peak magnitudes estimated using a distance of 34.25 Mpc and a reddening correction for an $E(B-V)$ of 0.112 mag are listed in Table 4. The errors in the absolute magnitudes have been estimated using uncertainties in the peak magnitude and the distance modulus of the host galaxy. Comparing the absolute magnitude of SN 2009jf with the absolute magnitude distribution of other SNe Ib (Richardson, Branch & Baron 2006, and references therein), SN2009jf lies close to the mean of the distribution. It is fainter than the extremely luminous SN Ib SN 1991D (Maza & Ruiz 1989) and comparable in brightness to SN 1984L, SN1990I (Elmhamdi et al. 2004), SN1999ex (Stritzinger et al. 2002; Hamuy et al. 2002) and SN 2000H (Krisciunas & Rest 2000). SN 2009jf is ∼1.5 mag brighter than SN 2007Y (Stritzinger et al. 2009) and ∼1 mag brighter than SN 2008D, which was associated with the X-ray transient 080909 (Modjaz et al. 2009).

The quasi-bolometric light curve of SN 2009jf is estimated using the reddening-corrected *UBVRI* magnitudes presented here. The reddening-corrected magnitudes were converted to monochromatic fluxes using the zero-points from Bessell, Castelli & Plez (1998). The quasi-bolometric fluxes were derived by fitting a spline curve to the U, B, V, R and I fluxes and integrating over the wavelength range from 3100 Å to 1.06 μm, determined by the response of the filters used. There are a few missing magnitudes in the U-band light curve, which were estimated by interpolating between the neighbouring points. The quasi-bolometric light curve of SN 2009jf plotted in Fig. 5 is compared with the bolometric light curves of SNe Ib SN 2008D, SN 2007Y, SN 1999ex, Type Ic supernova SN 1994I and broad-lined Type Ic SN 1998bw, also plotted in the figure. The bolometric light curves of supernovae SN 2008D, SN 2007Y, SN 1999ex and SN 1994I were constructed in a manner similar to SN 2009jf. The bolometric light curves of SN 2007Y (Stritzinger et al. 2009), SN 1999ex (Stritzinger et al. 2002) and SN 1994I (Richmond et al. 1996) are based on the published *UBVRI* magnitudes, while the bolometric light curve of SN 2008D includes the *Swift* UVOT (U band) and near-infrared (NIR) data also (Tanaka et al. 2009). The bolometric light curve of SN 1998bw is taken from Patat et al. (2001) which includes optical and NIR data. A total reddening $E(B-V)$ of 0.45, 0.3, 0.11, 0.65, 0.06 mag and distances of 8.32, 48.31, 19.31 31.0 and 37.8 Mpc were adopted for SN 1994I, SN 1999ex, SN 2007Y, SN 2008D and SN 1998bw, respectively.

The bolometric light curve of SN 2009jf is fainter than that of SN 1998bw and brighter than all other Type Ib/c supernovae in comparison. Adding a conservative uncertainty of ±0.2, mainly due to the uncertainty in H_0, the peak bolometric magnitude for SN 2009jf is estimated as −17.48 ± 0.2 mag, which is ∼1.4 mag brighter than SN 2007Y and ∼0.4 mag brighter than SN 1999ex. The contribution of NIR and UV fluxes to the bolometric flux for Type Ib/c

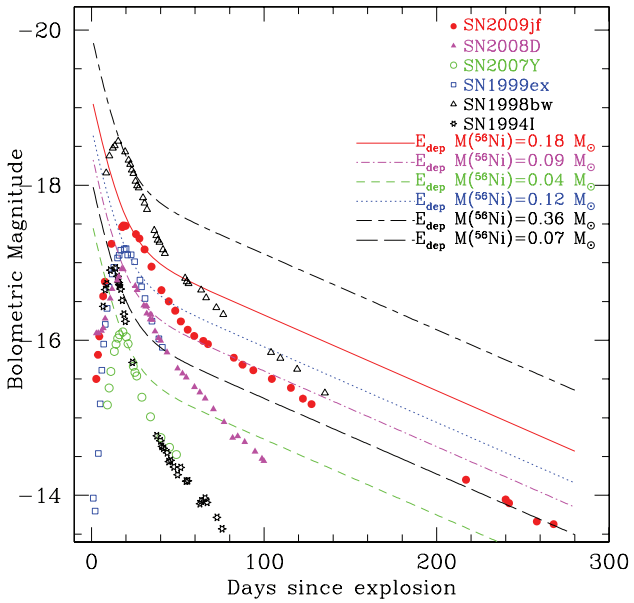

Figure 5. Bolometric light curve of SN 2009jf. Also plotted in the figure, for comparison, are the bolometric light curves of SN 2008D, SN 1999ex, SN 1998bw, SN 2007Y and SN 1994I. The continuous curves correspond to the rate of energy production for different masses of ^{56}Ni synthesized during the explosion, based on the analytical formulation by Nadyozhin (1994).

supernovae is not well constrained. For SN 2007Y, Stritzinger et al. (2009) have estimated that close to the peak brightness, ∼70 per cent of the flux is in the optical bands, ∼25 per cent in the UV bands and ∼5 per cent in the NIR bands. However, by two weeks past maximum, the UV contribution comes down to <10 per cent and NIR contribution rises up to ∼20 per cent. In the case of SN 2008D, the bolometric flux has an NIR contribution of about <24 per cent at ∼12 d after maximum light in *V* (Modjaz et al. 2009). Thus, the UV and NIR bands, together, contribute as much as ∼30 per cent to the bolometric flux. Even without considering the UV and NIR contribution to the bolometric light curve, it is seen that SN 2009jf is 0.6 mag brighter than SN 2008D at peak. Further, as seen in the *UBVRI* light curves, the decline rate of the bolometric light curve of SN 2009jf is slower than other supernovae in comparison. While the initial decline rate of SN 2009jf is comparable to that of SN 2008D, it is much slower than SN 2008D in the later phases. The slope of the bolometric light curve ∼45 d after *B* maximum is found to be 0.013 mag d^{-1}. For SN 2008D, the same quantity is 0.023 mag d^{-1}.

The mass of ^{56}Ni synthesized during explosion can be estimated following the principle that the bolometric luminosity, $L_{\rm bol}$, at maximum light is proportional to the instantaneous rate of radioactive decay (Arnett 1982). The simplified formulation of Arnett's rule, to estimate the mass of ^{56}Ni, $M_{\rm Ni} = L_{\rm bol}/\alpha\dot{S}$, as proposed by Nugent et al. (1995), involves α, the ratio of bolometric to radioactivity luminosity, and $\dot{S}$, the radioactivity luminosity per unit nickel mass, which depends on the rise time of the supernova to maximum light. The peak *UBVRI* bolometric luminosity for SN 2009jf is estimated as $3^{+0.6}_{-0.5} \times 10^{42}$ erg s^{-1}; the quoted uncertainty is mainly due to the uncertainty in H_0. SN 2009jf was discovered around 17.5 d before maximum in the *B* band, indicating that the minimum rise time is around 18 d. Assuming a rise time of 19 ± 1 d, the mass of ^{56}Ni is estimated to be $0.16^{+0.03}_{-0.03}$ M$_\odot$ for SN 2009jf. It is worth mentioning here that α, the ratio of bolometric to radioactivity luminosity, which takes into account the possible radiation transport effects, is assumed to be unity.

Another way for estimating the mass of ^{56}Ni synthesized during the explosion is to fit the energy deposition rate, via the ^{56}Ni → ^{56}Co chain, to the observed bolometric light curve. The total rate of energy production via the ^{56}Ni → ^{56}Co chain estimated using the analytical formula by Nadyozhin (1994), for different values of mass of ^{56}Ni synthesized during the explosion, is plotted with the bolometric light curves in Fig. 5. The energy deposition rate corresponding to a ^{56}Ni mass of 0.18 M$_\odot$ fits the initial decline of the quasi-bolometric light curve of SN 2009jf. The mass of ^{56}Ni estimated using Arnett's law and the energy deposition rate are in good agreement with each other, and in what follows, an average of the two estimates, 0.17 M$_\odot$, is taken as the mass of ^{56}Ni synthesized in the explosion. In the above estimates of ^{56}Ni mass, the contribution from UV and NIR bands to the bolometric luminosity has not been included. As discussed earlier, the contribution from UV and NIR bands to the bolometric luminosity at any given time is about 30 per cent. Including this contribution to the bolometric luminosity, the estimated mass of ^{56}Ni synthesized in the explosion will increase by ∼30 per cent.

6 SPECTRAL EVOLUTION

Our spectroscopic observations began 15 d before *B* maximum and continued till 99 d after *B* maximum, when the object went in solar conjunction. Subsequently, two spectra were obtained in the nebular phase, at 229 and 251 d after *B* maximum.

6.1 Early phase

The spectral evolution of SN 2009jf is plotted in Figs 6–8. Our first spectrum is one of the earliest spectra for SNe Ib, along with SN 2007Y (Stritzinger et al. 2009) and SN 2008D (Modjaz et al. 2009). All spectra have been corrected for the heliocentric velocity of 2381 km s^{-1} of the host galaxy. The pre-maximum spectra of SN 2009jf are plotted in Fig. 6. These spectra are characterized by a broad P-Cygni profile, indicative of high expansion velocity of the ejecta. The first spectrum taken on JD 245 5104.16 (15 d before *B* maximum) shows distinctive broad absorption due to He I

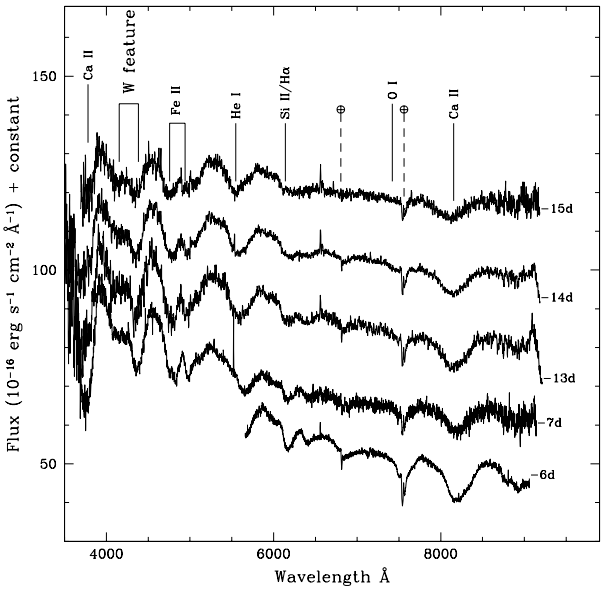

Figure 6. Pre-maximum spectral evolution of SN 2009jf during −15 to −6 d with respect to maximum in the *B* band.

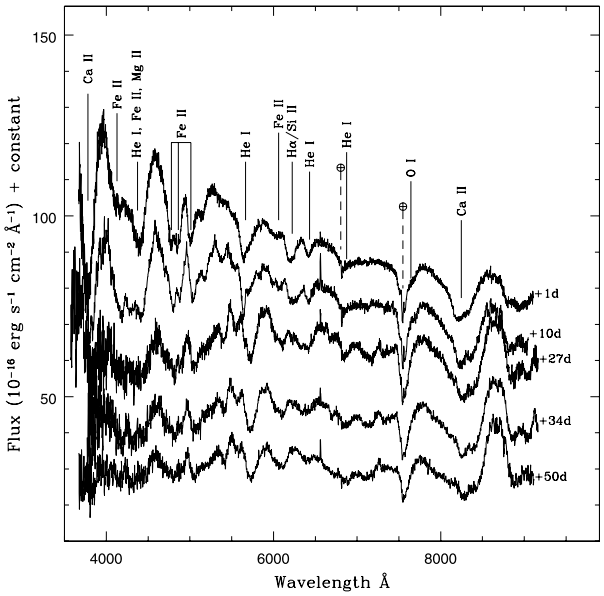

Figure 7. Spectral evolution of SN 2009jf around maximum and immediate post-maximum phase.

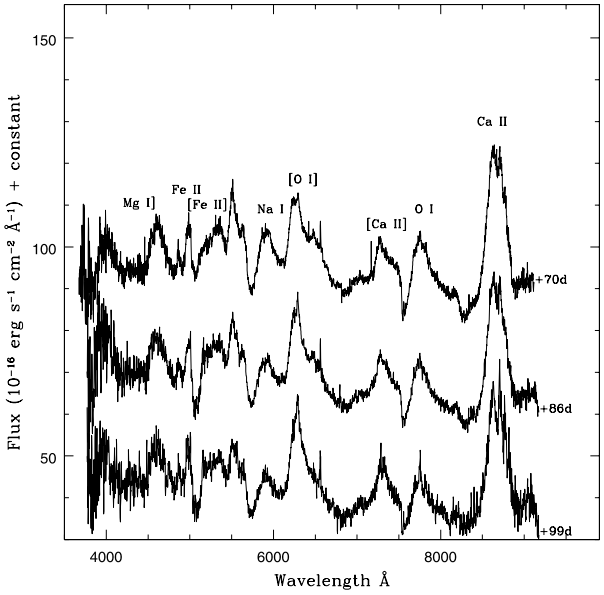

Figure 8. Spectral evolution of SN 2009jf during +70 to +99 d with respect to maximum in the *B* band.

5876 Å with an expansion velocity of ∼16 300 km s^{-1} and possible contribution from Na I D 5890, 5896 Å. The other well-developed features seen in the first spectrum are due to Ca II H&K 3934, 3968 Å ; Fe II between 4100 and 5000 Å ; Si II/Hα at ∼6250 Å ; O I 7774 Å and the Ca II NIR triplet between 8000 and 9000 Å. A clear signature of other He I lines 4471 Å (possibly blended with Fe II 4924 Å and Mg II 4481 Å), 5015, 6678 and 7065 Å is present in the spectrum taken ∼13 d before *B* maximum. The He I 7065 Å line is affected by the telluric H_2O band. The first spectrum also shows the double absorption, the 'W' feature, at ∼4000 Å seen in the very early spectra of the Type II supernova SN 2005ap (Quimby et al. 2007), the SN Ib SN 2008D (Modjaz et al. 2009) and the SN IIb SN 2001ig (Silverman et al. 2009). This feature is identified with Fe complexes (Mazzali et al. 2008) or as a combination of C III, N III and O III lines at high velocities (Modjaz et al. 2009; Silverman et al. 2009). Tanaka et al. (2009) have investigated the presence of C III, N III and O III lines in the early spectrum of SN 2008D using a Monte Carlo spectrum synthesis code and did not find a large contribution from these ionization states. They concluded that ionization by the photospheric radiation only is not enough for the observed features to be due to these doubly ionized lines.

The continuum becomes bluer as the supernova evolves towards maximum, as also indicated by the colour curves (Fig. 4).

The pre-maximum spectra of SN 2009jf are compared with those of SN 2007Y and SN 2008D at similar epochs and are shown in Fig. 9. The spectrum of SN 2009jf at 15 d before *B* maximum (top panel) shows well-developed absorptions at 4100–5500 Å due to Fe II and He I 5876 Å. In comparison, SN 2008D shows a nearly featureless spectrum around the same time. While the Fe II features are clearly identifiable in SN 2007Y, the He I 5876 Å feature is absent. The spectra of SN 2009jf and SN 2007Y at ∼7 d before *B* maximum (bottom panel) are very similar, except for the differences in the expansion velocities, while in SN 2008D, lines due to He I are identified, but Fe II lines are still not well developed.

The post-maximum spectra are shown in Figs 7 and 8. The spectrum of SN 2009jf obtained 1 d after *B* maximum shows a bluer continuum, with well-developed lines due to Ca II H&K, He I, Fe II and a broad P-Cygni profile of the Ca II NIR triplet. The prominent absorption at ∼6250 Å in the pre-maximum phase weakens and is not seen in the spectra beyond day +10. The continuum of the post-maximum spectrum on day +27 again becomes redder. Later on, the evolution of the spectrum is slow, with further suppression of the flux in blue and an increase in the flux of the Ca II NIR triplet.

The spectra of SN 2009jf, SN 2007Y and SN 1999ex close to maximum are plotted in Fig. 10 (top panel). The main features in the spectra are identified and marked in the figure. While the general characteristics of the spectrum in the three SNe are similar, it is seen that the Fe II lines around ∼5000 Å are somewhat underdeveloped in SN 1999ex. In the phase of ∼10 d after *B* maximum (Fig. 10, bottom panel), the spectral features in SN 2009jf appear to be narrower

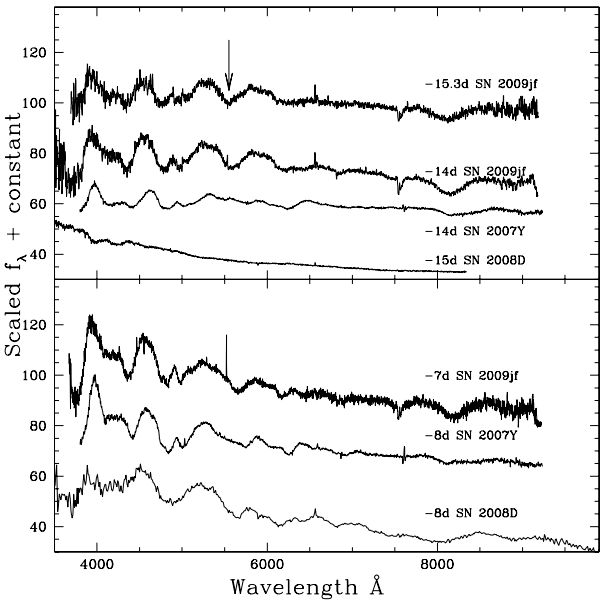

Figure 9. Comparison of pre-maximum spectra of SN 2009jf with SN 2008D and SN 2007Y. Note the early emergence of the He I line in SN 2009jf, marked by an arrow.

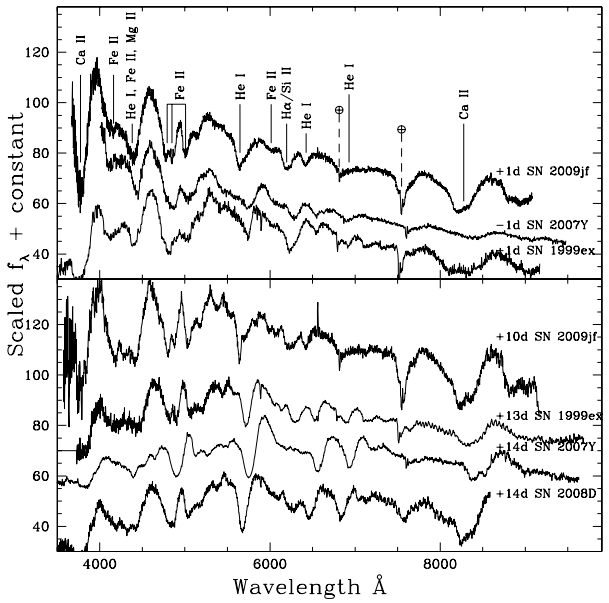

Figure 10. Spectral comparison of SN 2009jf around maximum and immediate post-maximum phase.

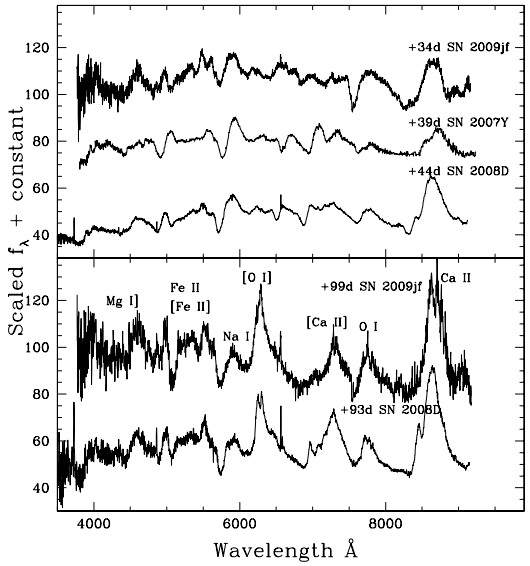

Figure 11. Spectral comparison of SN 2009jf at later phases.

compared to the other supernovae. Around a month after maximum, all three supernovae show identical features (Fig. 11, top panel).

Forbidden emission lines of [O I] 6300–6364 Å and [Ca II] 7291, 7324 Å are seen in the spectrum of day +70 (Fig. 8), marking the onset of the nebular phase. The spectra of +86 and +99 d after *B* maximum show a strengthening of the [O I] and [Ca II] features. The other features identified in these spectra are Mg I] 4570 Å, [Fe II] blend at 5200 Å, Na I doublet 5890, 5896 Å, O I 7774 Å and the blend at ∼8700 Å, which has contributions from O I 8446 Å, Ca II 8498–8662 Å and [C I] 8727 Å (Fransson & Chevalier 1989). The features have been identified in Fig. 11 (bottom panel). The [O I] profile at this phase is single peaked and asymmetric, with the emission peaking redwards. The asymmetry is more evident in the spectrum of day +99. In comparison, the +93-d spectrum of SN 2008D shows a symmetric double-peaked [O I] line.

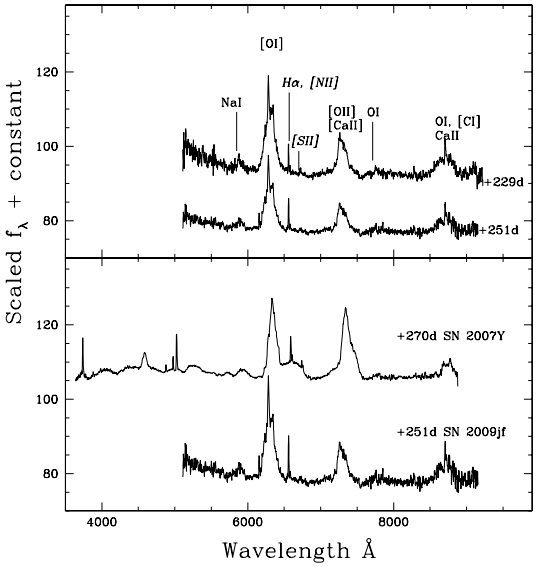

Figure 12. The top panel shows the nebular spectra of SN 2009jf. Hα+[N II] and [S II] features (marked in *italics*) from the underlying H II region are also identified in the spectra. The bottom panel shows the comparison with the nebular spectrum of SN 2007Y.

6.2 Nebular phase

The spectra taken 229 and 251 d after maximum are presented in Fig. 12. The spectrum during these days is dominated by the [O I] and [Ca II] features. The [Ca II] emission is blended with [Fe II] lines at 7155, 7172, 7388 and 7452 Å and possibly with [O II] 7320, 7330 Å (Stritzinger et al. 2009). The Na I 5890, 5896 Å doublet, O I 7774 Å and the 8700 Å blend are also identified in these spectra, but with a decreased strength compared to the spectra of 86 and 99 d after maximum. The FWHM of a Gaussian fit to the [O I] emission line indicates a velocity dispersion of ∼7300 km s^{-1}, whereas the corresponding velocity dispersion estimated for the [Ca II] line is ∼6500 km s^{-1}. The FWHM velocities measured for SN 2009jf are higher than those for SN 2007Y (Stritzinger et al. 2009), SN 1996N (Sollerman et al. 1998), SN 1985F (Schlegel & Krishner 1989) and the sample of SNe Ib discussed in Matheson et al. (2001), at similar epochs. The blend at ∼8700 Å has an FWHM of ∼8000 km s^{-1} on day +229, which decreases to ∼7300 km s^{-1} on day +251. The Ca II NIR/[Ca II] line ratio measured in the two nebular spectra indicates that the Ca II NIR is getting weaker as compared to the [Ca II] line, a feature noticed in SN 1996N (Sollerman et al. 1998) and interpreted as due to decreasing density (Filippenko, Porter & Sargent 1990). However, the blend at 8700 Å has contribution from O I, Ca II and [C I]; hence, the measured velocity and flux using this blend must be viewed with caution.

The emission-line profiles are multipeaked and asymmetric. The [O I] line shows a sharp and stronger blue peak. A similar profile is clearly apparent in the [Ca II] line of day +229. The sharp emission component appears to be present in all the emission lines. In addition to the broad features due to the supernova ejecta, the nebular spectra also show narrow lines due to Hα, [N II] 6548, 6583 Å and [S II] 6717, 6731 Å, originating from the underlying H II region.

6.3 Expansion velocity of the ejecta

Expansion velocities of the prominent features seen in the spectra are estimated by fitting a Gaussian profile to the minimum of the

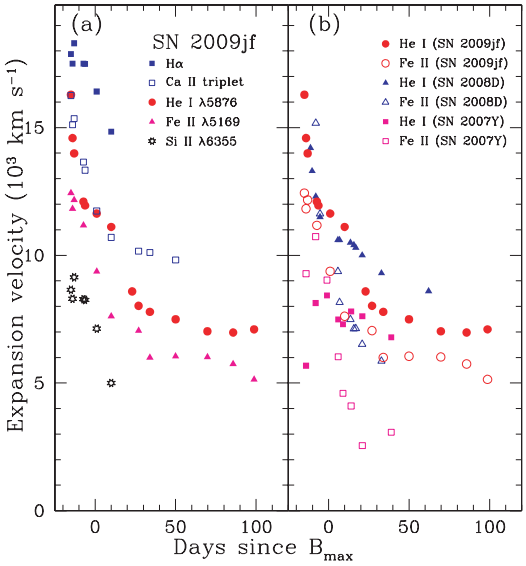

Figure 13. (a) Temporal velocity evolution of the prominent ions in SN 2009jf spectra. (b) Comparison of the He I and Fe II line velocities in SN 2009jf with those observed in SN 2007Y and SN 2008D.

absorption trough in the redshift-corrected spectra. The velocity evolution of the prominent ions, seen in the spectra of SN 2009jf, is plotted in Fig. 13(a). The expansion velocity of the He I 5876 Å line, determined using the pre-maximum spectra, rapidly decreases from a value of ∼16 000 km s^{-1} on day −15 to ∼12 000 km s^{-1} close to *B* maximum. The velocity further declines in the post-maximum phase and levels off at ∼7000 km s^{-1}. The expansion velocity of the Fe II 5169 Å feature remains low as compared to that of the He I 5876 Å line all through its evolution and also declines at a slower rate, as seen in most SNe Ib (Branch et al. 2002). The expansion velocities of the Ca II NIR triplet follow the evolution of the He I 5876 Å line, with a marginally higher velocity in the pre-maximum phase. While the velocity of the He I line decreases to ∼7000 km s^{-1} in the post-maximum phase, the velocity of the Ca II NIR triplet remains higher at ∼10 000 km s^{-1}.

The feature seen at 6250 Å in the spectra of some SNe Ib has been identified with Hα in SN 1954A, SN 1999di, SN 2000H (Branch et al. 2002) and SN 2005bf (Anupama et al. 2005), or with Si II in SN 1999ex (Hamuy et al. 2002), or as a blend of C II 6580 Å and Hα in SN 1999dn (Deng et al. 2000) or as a blend of Si II and Hα in SN 2008D (Tanaka et al. 2009). In the case of SN 2005bf, identification of the 6250 Å feature with Hα was supported by the presence of a blueshifted Hβ line in the early spectrum (Anupama et al. 2005). Similarly, in SN 2007Y, Stritzinger et al. (2009) have identified the 6250 Å feature with Hα possibly blended with Si II based on the presence of Hα in the nebular spectrum and a possible presence of Hβ in the early spectrum. The presence of a high-velocity Hα feature in the early phase is usually accompanied by the presence of a broad shoulder redward of the [O I] 6300–6364 Å feature, as seen in the spectrum of SN 2007Y. The presence of Hα absorption at early times and strong Hα emission in the late phase led Maurer et al. (2010) to reclassify SN 2007Y as Type IIb. Identifying the feature seen at 6250 Å in the spectra of SN 2009jf with Hα indicates expansion velocities much higher than He I, while identification with Si II indicates velocities that are lower than Fe II (see Fig. 13). Further, in the nebular spectra of SN 2009jf presented here, the broad shoulder redward of the [O I] 6300–6364 Å feature is also not seen. We therefore prefer to identify the 6250 Å feature with Si II.

The He I 5876 Å and Fe II 5169 Å line velocities estimated for SN 2009jf are compared with those of SN 2008D and SN 2007Y in Fig. 13(b). The velocity evolution of SN 2009jf is similar to that of SN 2008D. The He I velocity in both these objects is higher than the Fe II line velocity, whereas SN 2007Y has a higher Fe II velocity (Stritzinger et al. 2009). The He I velocity in SN 2009jf during the pre-maximum and early post-maximum phases is higher than SN 2008D, but ∼20 d after *B* maximum, the velocity in SN 2009jf becomes lower than SN 2008D. On the other hand, the Fe II line velocity is initially lower in SN 2009jf and becomes similar to SN 2008D at later epochs. SN 2007Y has lower velocities compared to both SN 2009jf and SN 2008D at all phases.

7 OXYGEN MASS

The nebular spectra of SNe Ib are dominated by [O I] emission, considered as the prime cooling path during the late phases (Uomoto 1986; Fransson & Chevalier 1987). The absolute flux of this line can be used to estimate the mass of neutral oxygen producing the line emission, following the expression by Uomoto (1986):

$$M(\mathrm{O}) = 10^8 \times D^2 \times \mathrm{F}([\mathrm{O\,I}]) \times \exp(2.28/T_4), \quad (1)$$

where M(O) is the mass of neutral oxygen in M$_\odot$, D is the distance to the supernova in Mpc, F([O I]) is the flux of the [O I] line in erg s^{-1} and T_4 is the temperature of the oxygen emitting region in units of 10^4 K. The above equation holds in the high density regime ($N_e \geq 10^6$ cm^{-3}), which is met in the ejecta of SNe Ib (Schlegel & Krishner 1989; Gomez & Lopez 1994; Elmhamdi et al. 2004). An estimate of the temperature of the line emitting region can be made using the [O I] 5577/6300–6364 flux ratio. The [O I] 5577 Å line is not detected in the nebular spectrum of SN 2009jf. This implies a limit on the [O I] 5577/6300–6364 flux ratio of ≤0.1. At this limit, the emitting region should either be at a relatively low temperature ($T_4 \leq 0.4$) for the high density limit or be at a low electron density ($n_e \leq 5 \times 10^6$ cm^{-3}) if $T_4 = 1$ (Maeda et al. 2007).

Elmhamdi et al. (2004) estimated a temperature of ∼3200–3500 K for SN 1990I at ∼237 d after maximum light, using an upper limit of the flux of the [O I]λ5577 line, while Schlegel & Krishner (1989) have estimated the mass of oxygen in SNe Ib SN 1984L and SN 1985F by assuming $T_4 = 0.4$. In all cases, a density of $\gtrsim 10^6$ cm^{-3} is assumed. Assuming that the high density regime is valid for SN 2009jf also, a value of $T_4 = 0.4$ appears to be a good approximation. Using the [O I] flux of 3.74 × 10^{-14} erg s^{-1} cm^{-2} measured in the spectrum of day +251, and the assumed distance of 34.25 Mpc, the mass of oxygen is estimated to be 1.34 M$_\odot$. A weak line at ∼7750 Å is present in the nebular spectra of SN 2009jf and is identified with the O I 7774 Å line, following Mazzali et al. (2010). The presence of the O I 7774 Å line in the spectrum is indicative of the presence of ionized oxygen also, as this line is mainly due to recombination (Begelman & Sarazin 1986). Mazzali et al. (2010) have shown that the mass of oxygen required to produce [O I] 6300–6364 Å and O I 7774 Å lines together is higher than what is required to produce only the [O I] 6300–6364 Å line. Thus, the oxygen mass estimate of 1.34 M$_\odot$ may be considered as a lower limit of the total mass of oxygen ejected during the explosion.

8 DISCUSSION

The light curve and spectral evolution of SN 2009jf show some peculiarities compared to other SNe Ib. The light curves indicate

a post-maximum decline that is slower compared to other SNe Ib. This slow decline continues even during the late phases, making the light curve of SN 2009jf broad. The absolute V magnitude at peak is comparable to the mean of the absolute magnitude distribution of SNe Ib. Using the bolometric light curve and the energy deposition rate via $^{56}\mathrm{Ni} \rightarrow {}^{56}\mathrm{Co}$, the mass of ^{56}Ni synthesized during the explosion is estimated to be $0.17\,\mathrm{M}_{\odot}$. SN 2009jf shows a very early emergence of He I lines in the spectrum. The He I 5876 Å line is identified in the first spectrum obtained 15.3 d before B maximum. Other lines due to He I at 4471 and 6678 Å were identified in the −13 d spectrum. Further, the expansion velocity estimated using the He I line is $\sim$16 000 km s^{-1}, indicating that helium is excited at high velocity. In the case of SN 2008D, He I lines became apparent around 11.5 d before B maximum and were prominent only around 5 d before B maximum (Modjaz et al. 2009). The He I lines seen in the spectra of SNe Ib require non-thermal excitation and ionization, as the temperature present in the ejecta is too low to cause any significant absorption (Lucy 1991). γ-rays, emitted by newly synthesized ^{56}Ni during the explosion, accelerate electrons that act as a source of non-thermal excitation for He (Harkenss et al. 1987; Lucy 1991). For exciting helium at such a high velocity as seen in SN 2009jf, the γ-rays need to be close to the helium layer, which can be possible either through the escape of γ-rays from the ^{56}Ni-dominated region or through some large-scale instability causing substantial mixing of ^{56}Ni with the outer layers. The slower decline of the light curves of SN 2009jf gives an indication that it has a massive ejecta and the probability of γ-rays escaping will be low. Though substantial mixing of different inner layers appears to be the most probable way for an early excitation of He at high velocities, the possibility of some γ-rays reaching the He layer and exciting it cannot be ruled out, especially since SN 2009jf is a rather luminous supernova.

The profile of the [O I] 6300–6364 Å feature in the nebular spectrum is multipeaked and asymmetric with a sharp, stronger blue peak. The peak of this feature is blueshifted by $\sim$30 Å around day +86, which reduces to a blueshift of $\sim$15 Å by day +99. Such observed blueshifts are explained as a result of residual opacity in the core of the ejecta (Taubenberger et al. 2009). The asymmetric and multipeaked profile seen at phases later than 200 d can be produced by additional components of arbitrary width and shift with respect to the main component. Such profiles are indicative of an ejecta with large-scale clumping, a single massive blob or a unipolar jet. The asymmetric [O I] line profile of SN 2009jf with a stronger blue peak is very similar to the line profiles of SNe 2000ew and 2004gt. Taubenberger et al. (2009) have explored a possible configuration which can give rise to this asymmetric line profile and interpreted the profile as originating from the deblended 6300 and 6364 Å lines of a single narrow, blueshifted component. Maurer et al. (2010) have shown that the profile of the [O I] 6300–6364 Å doublet is likely to be influenced by Hα absorption. If hydrogen concentration is located around $\sim$12 000 km s^{-1}, it causes a split of the [O I] 6300–6364 Å doublet, leading to a double-peaked oxygen profile. Neither scenarios account for the stronger blue peak of the 6300-Å line. Taubenberger et al. (2009) explained the stronger blue peak with a complex ejecta structure with additional blueshifted emission on top of an otherwise symmetric profile. Alternatively, the asymmetry in the profile is explained by a damping of the redshifted emission component in an originally toroidal distribution, caused by the optically thick inner ejecta. The light-curve evolution of SN 2009jf indicates the presence of an ejecta more massive than other stripped core-collapse supernovae. Hence, it is quite likely that in the case of SN 2009jf also the redward component is damped by an optically thick inner ejecta. It should, however, be noted that asymmetric and multicomponent profiles cannot be reproduced within spherical symmetry (Mazzali et al. 2005; Maeda et al. 2007). This needs further investigation with observations at phases later than presented here, as well as spectrophotometric observations and detailed modelling.

The brightness and width of Type Ib light curves are determined by the interplay of nickel mass, opacity and γ-ray deposition. In general, a greater amount of ^{56}Ni will make the light curve brighter. A more massive ejecta will have a larger optical depth, and it will take longer for the trapped decay energy to diffuse through the envelope, which will broaden the light curve (Ensman & Woosley 1988). The time taken for the bolometric light curve to decline from peak to the moment when the luminosity is equal to $1/e$ times the peak luminosity (which is equivalent to a decline of 1.1 mag from peak) is known as the effective diffusion time τ_{m}. The effective diffusion time is related to the mass of the ejecta M_{ej} and the kinetic energy E_{k} of the ejecta $\tau_{\mathrm{m}} \propto \kappa_{\mathrm{opt}}^{1/2} M_{\mathrm{ej}}^{3/4} E_{\mathrm{k}}^{-1/4}$ (Arnett 1982), where κ_{opt} is the optical opacity. The expansion velocity v can be expressed in terms of M_{ej} and E_{k} as $v \propto M_{\mathrm{ej}}^{-1/2} E_{\mathrm{k}}^{1/2}$. The broad peak and slower decline rates of the light curves of SN 2009jf in comparison to other supernovae indicate that SN 2009jf has a massive ejecta. Further, the broader emission lines at a late phase indicate a larger explosion energy.

There are several core-collapse supernovae for which the progenitor mass has been constrained using hydrodynamical modelling. With this approach, Nomoto et al. (2003, 2004) constructed the E_{K}–M_{MS} diagram and introduced a hypernova branch. Recent updates of this approach include SN 1998bw (Maeda, Mazzali & Nomoto 2006), SN 2008D (Tanaka et al. 2009) and SN 2003bg (Mazzali et al. 2009). For the well-studied bright hypernova SN 1998bw ($M_V = -19.35$; Galama et al. 1998), the main-sequence mass of the progenitor is constrained by Maeda et al. (2006) as $\sim 40\,\mathrm{M}_{\odot}$. Though SN 2009jf has a brighter peak compared to SN 2008D, the fact that the light curves of SN 2009jf around maximum and the initial decline rate $\Delta m_{15}(V)$ are similar to those of SN 2008D can be used to estimate the mass of the ejecta M_{ej} and kinetic energy E_{k} of the ejecta, using SN 2008D as the reference, assuming the optical opacity κ_{opt} to be the same. The effective diffusion times τ_{m} for SN 2009jf and SN 2008D are estimated to be 30 and 26 d, respectively. The photospheric expansion velocity estimated using the Fe II 5169 Å line at maximum is $\sim$10 000 km s^{-1}, similar for both the objects. For SN 2008D, the mass of the ejecta M_{ej}, the kinetic energy E_{k} and the progenitor mass have been derived by Mazzali et al. (2008), Soderberg et al. (2008) and Tanaka et al. (2009), respectively. Mazzali et al. (2008) could reproduce the spectral evolution and light curve with a spherically symmetric explosion energy $E_{\mathrm{k}} = 6.0 \times 10^{51}$ erg and ejected mass $M_{\mathrm{ej}} \sim 7\,\mathrm{M}_{\odot}$ with a progenitor mass of $\sim 30\,\mathrm{M}_{\odot}$, while Soderberg et al. (2008) have arrived at $E_{\mathrm{k}} = 2$–4×10^{51} erg and $M_{\mathrm{ej}} = 3$–$5\,\mathrm{M}_{\odot}$ by applying rescaling arguments. Tanaka et al. (2009) have calculated the hydrodynamics of explosion and explosive nucleosynthesis for SN 2008D with varying masses for the He core of the progenitor and concluded that the progenitor star of SN 2008D had an He core mass of 6–8 $\mathrm{M}_{\odot}$ prior to explosion. This corresponds to a main-sequence mass of $M_{\mathrm{MS}} = 20$–$25\,\mathrm{M}_{\odot}$. The explosion energy and mass of ejecta for SN 2008D were estimated to be $E_{\mathrm{k}} = 6.0 \pm 2.5 \times 10^{51}$ erg and $M_{\mathrm{ej}} = 5.3 \pm 1.0\,\mathrm{M}_{\odot}$, respectively. Thus, for SN 2008D the mass of ejecta M_{ej} and explosion energy E_{k} range between 3–7 $\mathrm{M}_{\odot}$ and 2–6 $\times\ 10^{51}$ erg, respectively. Using the observed photospheric velocity and the estimated diffusion time for SN 2009jf, and treating SN 2008D as a reference, we estimate

$M_{ej} = 4$–$9\,M_\odot$ and $E_k = 3$–8×10^{51} erg for SN 2009jf. This indicates that SN 2009jf was an energetic explosion of a star having a mass similar to, or somewhat more massive than, the progenitor of SN 2008D ($M_{MS} \gtrsim 20$–$25\,M_\odot$). The physical parameters of SN 2009jf may also be compared with those of the Type IIb supernova SN 2003bg, which had an absolute peak magnitude of $M_V = -17.5$ (Hamuy et al. 2009) and an oxygen mass estimate of $1.3\,M_\odot$. Mazzali et al. (2009) have estimated the physical parameters for SN 2003bg based on detailed light curve and spectral modelling. The best-fitting model gives an ejected mass of $\sim 4.8\,M_\odot$, kinetic energy of $\sim 5 \times 10^{51}$ erg and mass of ^{56}Ni ~ 0.15–$0.17\,M_\odot$. The mass of the progenitor for SN 2003bg is estimated as 20–$25\,M_\odot$. Our qualitative analysis of light curve and spectra of SN 2009jf hints towards a higher kinetic energy and a slightly more massive ejecta than SN 2003bg, and in turn a progenitor with $M_{MS} \gtrsim 20$–$25\,M_\odot$.

The mass of oxygen M(O) in the ejecta of the core-collapse SNe is very sensitive to the main-sequence mass M_{MS} of the progenitor. For $M_{MS} = 15$, 18, 20, 25, 30 and $40\,M_\odot$, $M(O) = 0.16$, 0.77, 1.05, 2.35, 3.22 and $7.33\,M_\odot$, respectively (Nomoto et al. 2006). These values are obtained for $E_k = 1.0 \times 10^{51}$ erg and the metallicity $z = 0.02$, but are not so sensitive to E_k and z. In fact, for ($M_{MS}/M_\odot$, $E_k/10^{51}$ erg) = (20, 10), (25, 10), (30, 20) and (40, 30), $M(O)/M_\odot = 0.98$, 2.18, 2.74 and 7.05, respectively (Nomoto et al. 2006). Therefore, the lower limit of the oxygen mass $M(O) \gtrsim 1.34\,M_\odot$ estimated from the nebular spectra is quite consistent with the progenitor mass of $M_{MS} \gtrsim 20$–$25\,M_\odot$ estimated from the light-curve shape and the photospheric velocities.

The [Ca II] 7291-7324/[O I]6300–6364 line ratio is also a good diagnostic of M_{MS}, because the mass of the explosively synthesized Ca in the ejecta, M(Ca), is not sensitive to M_{MS}. For $M_{MS}/M_\odot = 15$, 18, 20, 25, 30 and 40, $M(Ca)/10^{-2}\,M_\odot = 0.40$, 0.45, 0.37, 0.66, 1.6 and 1.6, respectively (Nomoto et al. 2006). Also, for ($M_{MS}/M_\odot$, $E_k/10^{51}$ erg) = (20, 10), (25, 10), (30, 20) and (40, 30), $M(Ca)/10^{-2}\,M_\odot = 0.50$, 0.57, 0.93 and 1.4, respectively (Nomoto et al. 2006). This is in contrast to M(O), which sensitively increases with M_{MS}. Thus, a smaller [Ca II]/[O I] ratio indicates a massive core.

The [Ca II] 7291–7324/[O I]6300–6364 emission-line ratio for SN 2009jf is estimated as 0.51 and 0.49 using the nebular spectrum observed on days +229 and +251, respectively. For SN 2007Y, SN 1996N, SN 1990I and SN 1998bw, this ratio was found to be 1.0, 0.9, 0.7 and 0.5, respectively, at similar epochs (Elmhamdi et al. 2004; Stritzinger et al. 2009, and references therein). Fransson & Chevalier (1989) have theoretically calculated the [Ca II]/[O I] line ratio for progenitor masses of 15 and $25\,M_\odot$. The observed [Ca II]/[O I] ratio for SN 2009jf is very close to the ratio expected for a star with $M_{MS} = 25\,M_\odot$, as indicated by Model 1b in Fransson & Chevalier (1989).

The estimates of the mass of ^{56}Ni synthesized during the explosion, the kinetic energy of explosion and the main-sequence mass of the progenitor star place SN 2009jf between the normal core-collapse supernovae and the hypernovae branch in the E_K–M_{MS} diagram of Tanaka et al. (2009), at the upper end of the normal core-collapse supernovae branch. It is, however, to be noted that the [O I] line profile during the nebular phase indicates asymmetry of the explosion. This can have some effect in the kinetic energy estimate, as shown by Maeda et al. (2006) and Tanaka et al. (2007) for SN 1998bw. A detailed modelling is therefore required for a better estimate of the various parameters.

Itagaki et al. (2009) suggested that the progenitor could have undergone luminous blue variable-type mass-loss events, based on their detection of a dim object at the location of the supernova on three occasions. Pre-supernova images of the host galaxy obtained in the ultraviolet by the *Swift* satellite, and available in the *Swift* data archives, clearly indicate the presence of a bright H II region at the supernova location. It is hence quite likely that the object detected by Itagaki et al. (2009) corresponds to the underlying H II region.

9 SUMMARY

We present in this paper optical photometry and medium-resolution optical spectroscopy of the SN Ib SN 2009jf, spanning a period from ~ 15 d before B-band maximum to ~ 250 d post-maximum. SN 2009jf reached a B maximum on JD 245 5119.46, with an absolute magnitude $M_B = -17.58 \pm 0.19$. A slow post-maximum decline is indicated by the broad light curves. The peak bolometric flux implies that $\sim 0.17\,M_\odot$ of ^{56}Ni was synthesized during the explosion.

The spectral evolution of SN 2009jf is typical of the Type Ib class, but with an early emergence of helium lines. He I 5876 Å is clearly identified in the first spectrum obtained 15 d before maximum, at a velocity of $\sim 16\,000$ km s^{-1}. This early emergence of helium lines is likely due to a substantial mixing of the inner layers of the ejecta. The [O I] 6300–6364 Å line seen in the nebular spectrum is multipeaked and asymmetric, with a sharp, stronger blue peak. This is explained by the complex ejecta structure of an aspherical explosion. The absolute flux of this line indicates the mass of oxygen ejected during the explosion to be $\gtrsim 1.34\,M_\odot$.

A qualitative analysis of the light curve and spectra of SN 2009jf indicates that SN 2009jf is an energetic explosion of a massive star. The mass of the ejecta and kinetic energy of explosion are estimated to be $M_{ej} = 4$–$9\,M_\odot$ and $E_k = 3$–8×10^{51} erg, respectively. The main-sequence mass of the progenitor star is estimated to be $\gtrsim 20$–$25\,M_\odot$.

ACKNOWLEDGMENTS

We would like to thank the anonymous referee for the constructive comments, which helped in improving the paper. We thank all the observers of the 2-m HCT who kindly provided part of their observing time for the supernova observations. This work has been supported in part by the DST-JSPS grant DST/INT/JSPS/P-93/2010, the Grant-in-Aid for Scientific Research of JSPS (20540226) and MEXT (19047004, 22012003) and by World Premier International Research Center Initiative, MEXT, Japan. This work has made use of the NASA Astrophysics Data System and the NED which is operated by Jet Propulsion Laboratory, California Institute of Technology, under contract with the National Aeronautics and Space Administration.

REFERENCES

Anupama G. C., Sahu D. K., Deng J., Nomoto K., Tominaga N., Tanaka M., Mazzali P. A., Prabhu T. P., 2005, ApJ, 631, L125
Arnett W. D., 1982, ApJ, 253, 785
Begelman M. C., Sarazin C. L., 1986, ApJ, 302, L59
Berger E., Soderberg A. M., 2008, GCN Circular, 7159
Bessell M. S., Castelli F., Plez B., 1998, A&A, 333, 231
Branch D. et al., 2002, ApJ, 566, 1005
Deng J. S., Qiu Y. L., Hu J. Y., Hatano K., Branch D., 2000, ApJ, 540, 452
Elmhamdi A., Danziger I. J., Cappellaro E., Della Valle M., Gouiffes C., Phillips M. M., Turatto M., 2004, A&A, 426, 963
Elmhamdi A., Danziger I. J., Branch D., Leibundgut B., Baron E., Kirshner R. P., 2006, A&A, 450, 305
Ensman L. M., Woosley S. E., 1988, ApJ, 333, 754

Filippenko A. V., Porter A. C., Sargent W. L. W., 1990, AJ, 100, 1575
Fransson C., Chevalier R., 1987, ApJ, 322, L15
Fransson C., Chevalier R., 1989, ApJ, 343, 323
Galama T. J. et al., 1998, Nat, 396, 670
Gomez G., Lopez R., 1994, AJ, 108, 195
Hamuy M. et al., 2002, AJ, 124, 417
Hamuy M. et al., 2009, ApJ, 703, 1612
Harkenss R. P. et al., 1987, ApJ, 317, 355
Horne K., 1986, PASP, 98, 609
Itagaki K., Kaneda H., Yamaoka H., 2009, Central Bureau Electron. Telegrams, 1955, 3
Jester S. et al., 2005, AJ, 130, 873
Kasliwal M. M., Howell J. L., Fox D., Quimby R., Gal-Yam A., 2009, Astron. Telegram, 2218, 1
Krisciunas K., Rest A., 2000, IAU Circular, 7382
Landolt A. U., 1992, AJ, 104, 340
Leonard D. C. et al., 2006, Nat, 440, 505
Li L.-X., 2007, MNRAS, 375, 240
Li W., Cenko S. B., Filippenko A. V., 2009, Central Bureau Electron. Telegrams, 1952, 1
Lucy L. B., 1991, ApJ, 383, 308
Maeda K., Nakamura T., Nomoto K., Mazzali P. A., Patat F., Hachisu I., 2002, ApJ, 565, 405
Maeda K., Mazzali P. A., Nomoto K., 2006, ApJ, 645, 1331
Maeda K. et al., 2007, ApJ, 666, 1069
Martin R., Williams A., Woodings S., Biggs J. Verveer A., 1999, IAU Circular, 7310
Matheson T., Filippenko A. V., Li W., Leonard D. C., 2001, AJ, 121, 1648
Maurer I., Mazzali P. A., Taubenberger S., Hachinger S., 2010, MNRAS, 409, 1441
Maza J., Ruiz M. T., 1989, ApJS, 69, 353
Mazzali P. A., Nomoto K., Patat F., Maeda K., 2001, ApJ, 559, 1047
Mazzali P. A. et al., 2005, Sci, 308, 1284
Mazzali P. A. et al., 2008, Sci, 321, 1185
Mazzali P. A., Deng J., Hamuy M., Nomoto K., 2009, ApJ, 703, 1624
Mazzali P. A., Maurer I., Valenti S., Kotak R., Hunter D., 2010, MNRAS, 408, 87
Modjaz M. et al., 2009, ApJ, 702, 226.
Nadyozhin D. K., 1994, ApJS, 92, 527
Nomoto K., Suzuki T., Shigeyama T., Kumagai S., Yamaoka H., Saio H., 1993, Nat, 364, 507
Nomoto K., Maeda K., Umeda H., Ohkubo T., Deng J., Mazzali P., 2003, in Van der Hucht K. A., Artemio H., Esteban C., eds, Proc. IAU Symp. 212, A Massive Star Odyssey: From Main Sequence to Supernovae. Astron. Soc. Pac., San Francisco, p. 395
Nomoto K., Maeda K., Mazzali P. A., Umeda H., Deng J., Iwamoto K., 2004, in Fryer C. L., ed., Astrophysics and Space Science Library Vol. 302, Stellar Collapse. Kluwer, Dordrecht, p. 277
Nomoto K., Tominaga N., Umeda H., Kobayashi C., Maeda K., 2006, Nuclear Phys. A, 777, 424
Nugent P., Branch D., Baron E., Fisher A., Vaughan T., 1995, Phys. Rev. Lett., 75, 394
Patat F. et al., 2001, ApJ, 555, 900
Podsiadlowski P., Langer N., Poelarends A. J. T., Rappaport S., Heger A., Pfahl E., 2004, ApJ, 612, 1044
Quimby R. M., Aldering G., Wheeler J. C., Hoflich P., Akerlof C. W., Rykoff E. S., 2007, ApJ, 668, L99
Richardson D., Branch D., Baron E., 2006, AJ, 131, 2233
Richmond M. W., Treffers R. R., Filippenko A. V., Paik Y., Leibundgut B., Schulman E., Cox C. V., 1996, AJ, 111, 327
Sahu D. K., Anupama G. C., Gurugubelli U. K., 2009a, Central Bureau Electron. Telegrams, 1955, 2
Sahu D. K., Tanaka M., Anupama G. C., Gurugubelli U. K., Nomoto K., 2009b, ApJ, 697, 676
Schlegel E. M., Krishner R. P., 1989, AJ, 98, 577
Schlegel D. J., Finkbeiner D. P., Davis M., 1998, ApJ, 500, 525
Silverman J. M., Mazzali P., Chornock R., Filippenko A. V., Clocchiatti A., Phillips M. M., Ganeshlingam M., Foley R. J., 2009, PASP, 121, 689
Soderberg A. M. et al., 2008, Nat, 453, 469
Sollerman J., Leibundgut B., Spyromilio J., 1998, A&A, 337, 207
Stalin C. S., Hegde M., Sahu D. K., Parihar P. S., Anupama G. C., Bhatt B. C., Prabhu T. P., 2008, Bull. Astron. Soc. India, 36, 111
Stritzinger M. et al., 2002, AJ, 124, 2100
Stritzinger M. et al., 2009, ApJ, 696, 713.
Tanaka M., Maeda K., Mazalli P. A., Nomoto K., 2007, ApJ, 668, L19
Tanaka M. et al., 2009, ApJ, 692, 1131
Taubenberger S. et al., 2009, MNRAS, 397, 677
Uomoto A., 1986, ApJ, 310, L35
Wang L., Baade D., Hoflich P., Wheeler J. C., 2003, ApJ, 592, 457
Woosley S. E., Langer N., Weaver T. A., 1993, ApJ, 411, 823

This paper has been typeset from a TEX/LATEX file prepared by the author.